Open core threading dislocations in GaN grown by hydride vapour phase epitaxy

David Cherns, Michael Hawkridge

Open core threading dislocations in GaN grown by hydride vapour phase epitaxy

Journal:	*Philosophical Magazine & Philosophical Magazine Letters*
Manuscript ID:	TPHM-05-Dec-0553.R1
Journal Selection:	Philosophical Magazine
Date Submitted by the Author:	08-Mar-2006
Complete List of Authors:	Cherns, David; University of Bristol, Physics Hawkridge, Michael; University of Bristol, Physics
Keywords:	EELS, GaN, HAADF-STEM, TEM, dislocations
Keywords (user supplied):	

Open core threading dislocations in GaN grown by hydride vapour phase epitaxy

D. CHERNS and M.E. HAWKRIDGE

H.H. Wills Physics Laboratory, University of Bristol, Tyndall Avenue, Bristol BS8 1TL, UK

Abstract

Three types of threading dislocation in (0001) GaN films (c, c+a, and a-type) have been observed to have hollow cores, depending on the method of growth, and on the presence of electrical dopants or other impurities. In this paper, we discuss high resolution imaging and electron energy loss spectroscopy studies which show that open core screw dislocations in GaN films grown by hydride vapour phase epitaxy have surfaces that are substituted by oxygen. It is argued that open core formation is not primarily driven by the need to reduce strain field energy, but is influenced by kinetic factors, with oxygen stabilising the open core surfaces and acting as a growth inhibitor. It is pointed out that impurity segregation can explain a range of observed dislocation core structures in GaN. The significance of oxygen segregation for understanding the electronic properties of dislocations in GaN is briefly discussed.

Contact: Prof D. Cherns, email: d.cherns@bris.ac.uk, tel: +44(0)1179288702

Word count: 3264 words

1. Introduction

Semiconductor devices based on GaN/InGaN/AlGaN epitaxial layers are now of major economic importance, with applications ranging from highly efficient blue, green and white light emitting diodes (LEDs) and blue laser diodes (LDs) to electronic devices for high speed, high power applications. However, the performance of these devices is strongly influenced by high densities of threading dislocations, up to $10^9 cm^{-2}$, present in the active layers. The structure and optoelectronic properties of these threading dislocations, as well as mechanisms of dislocation reduction, have been much studied. The GaN/InGaN/AlGaN films grown for devices generally have the hexagonal wurtzite structure and are grown in (0001) orientation on substrates such as (0001) sapphire and SiC. They typically contain dislocations of three different types, with Burgers vector of 1/3<11-20> (a-type), 1/3<11-23> (a+c-type) and <0001> (c-type). Where the dislocations follow the [0001] growth axis (normally the case in unpatterned films), they are in edge, mixed and screw orientation respectively.

Transmission electron microscopy (TEM) studies of GaN structures have shown that, for the most part, threading dislocations have undissociated cores, although there is some evidence that a+c dislocations are dissociated on a fine scale [1]. In contrast, we have shown that screw dislocations, i.e. dislocations with <0001> Burgers vector, in undoped GaN films grown by metal-organic chemical vapour deposition (MOCVD), can have hollow cores with diameters of 20-50nm [2]. These are often termed "nanopipes". Since these early observations, the picture has become more complex. In Si-doped GaN films grown by MOCVD, it has been observed that screw dislocations can be open or closed core, and that, for open core dislocations, the core diameter can vary greatly [3]. In heavily Mg-doped AlGaN films grown by

Deleted: 1

Deleted: 2

MOCVD, edge and mixed dislocations were found to be open core [4]. While GaN films grown by molecular beam epitaxy (MBE) generally show dislocations of all types to be closed core, we have found that mixed and screw dislocations can be open core in films grown under extremely Ga-rich conditions [5].

Deleted: 3

Deleted: 4

The observation of hollow core dislocations is, of course, unusual in that the vast majority of TEM observations have shown that dislocation core relaxation occurs by dissociation into partials. However, it is interesting to note that, in a paper predating TEM studies of dislocations, Frank [6] proposed that dislocations with large Burgers vectors b might reduce their energy by forming hollow cores. This releases the strain energy associated with the highly distorted material close to the core at the expense of energy associated with the newly created surfaces. Frank's isotropic continuum model gave the equilibrium radius as

Deleted: 5

$$r = \mu b^2 / 8\pi^2 \gamma \qquad (1)$$

where μ, b, and γ are the shear modulus, Burgers vector and surface energy respectively. There is evidence that Frank's theory may explain the presence of micropipes observed in several other hexagonal materials [7]. Micropipes in (0001)SiC films have been most studied owing to their importance in electronic devices (e.g high power switches). They are associated with growth spirals, and have been confirmed as hollow core dislocations with large Burgers vectors (sometimes greater than 10nm) by atomic force microscopy (AFM) and by synchrotron radiation studies. While these studies only detect a screw component of Burgers vector, a detailed analysis of a range of data suggests that there is good quantitative agreement

Deleted: 6

with the Frank theory assuming that the Burgers vectors are of mixed type [8]. However, this has yet to be conclusively demonstrated experimentally.

Deleted: 7

In contrast, the Frank theory cannot satisfactorily account for hollow core dislocations in GaN. Firstly, screw dislocations in GaN have a Burgers vector of 0.52nm, which implies an equilibrium radius of near atomic dimensions using equation 1 and reasonable values of the surface energy [2]. However, Northrup [9] has suggested that the surface energy could be lowered, and the equilibrium radius increased, by the presence of impurities on the {10-10} nanopipe surfaces during growth. Secondly, the Frank theory implies that edge dislocations, which have the smallest Burgers vectors (b = 0.32nm, compared with 0.61nm (mixed) and 0.52nm (screw)), are least likely to form open cores. This is in disagreement with observations on Mg-doped material [4].

Deleted: 1

Deleted: 8

Deleted: 3

The varying observations reported in GaN-based films doped with Si, Mg and excess Ga suggest strongly, but indirectly, that impurities play a key role in nanopipe formation. Arslan and Browning [10] reported some direct evidence of oxygen segregation to nanopipes in MOCVD-grown GaN, using a combination of electron energy loss spectroscopy (EELS) and imaging in a scanning transmission electron microscope (STEM), although absolute amounts were not determined. In this paper, we discuss recent more quantitative studies of oxygen segregation, reported in brief recently [11]. We describe studies of nanopipes in GaN films grown by hydride vapour phase epitaxy (HVPE). By combining TEM with EELS and imaging in the STEM, it is shown that the nanopipe surfaces have nearly 2 monolayers of oxygen present. It is proposed that the oxygen is incorporated during growth and can explain both the formation of nanopipes, and the observed electronic properties of dislocations in GaN.

Deleted: results

Deleted: 9

Deleted: which confirm this link

Deleted: microanalysis by electron energy loss spectroscopy (EELS) and imaging in a scanning transmission electron microscope (STEM),

2. Experimental observations

Studies were carried out on GaN films of thicknesses 0.6, 5 and 55 µm grown by HVPE on (0001) sapphire at around 1100°C by R. Molnar (MIT). Films for TEM and STEM studies were prepared by mechanical polishing and ion thinning in plan-view and cross-sectional orientation. Films were subjected to plasma cleaning for STEM studies, using a Fischione Instruments Model 1020 cleaner with a 25%O_2/75%Ar gas mixture. TEM observations were mostly carried out in a Philips EM430 operating at 250kV. STEM observations were made in the Daresbury SuperSTEM which has aberration correctors giving a probe size down to 0.09nm, and in a FEI Titan 80-300 TEM with a probe size less than 0.16nm (without aberration correctors).

Formatted: Subscript

Nanopipes were observed in all three samples. In all cases, some nanopipes were uniformly open-core, i.e with a constant diameter, while others had alternately open and closed core segments. Figure 1 shows bright field TEM images of nanopipes in a cross-sectional sample, illustrating the variety of structures observed. The nanopipe in Figure 1(a) shows a uniform open core, while those in Figures 1(b), and Figure 1(c) (nanopipe *b*), show a more irregular structure. A few nanopipes were not associated with dislocations, and an example is labelled *n* in Figure 1(c). However, most nanopipes were associated with screw dislocations, with Burgers vectors **b** = [0001]. The dislocation character accounts for changes in diffraction contrast near the nanopipes in Figures 1 (other than *n*). The nature of the dislocations was confirmed by observing diffraction contours observed in bent regions of sample, or by large angle convergent beam electron diffraction (LACBED). An example is shown in Figure 2.

In this bright field image, the g = 0004 contour is seen to deviate and split on crossing a nanopipe. This splitting has been analysed in LACBED studies of dislocations [12], but applies equally well in images where the specimen is bent, as in Figure 2. The rule is that, if the number of subsidiary minima (dark peaks) in a bright field image is m, $\boldsymbol{g.b} = m + 1$. As $m = 3$ in Figure 2 (n.b. the middle peak crosses the nanopipe), we can deduce that the value of $\boldsymbol{g.b} = 4$, consistent with b = [0001].

High resolution images of nanopipes were obtained from plan-view samples by viewing approximately along [0001], i.e. along the nanopipe axis. Figure 3 shows a high angle annular dark field (HAADF) image taken on a FEI Titan 80-300 microscope operating at 300kV. The beam orientation is very close to [0001], such that the image shows reasonable 6-fold symmetry with atom columns 0.19nm apart resolved. Figure 4 shows results obtained on the Daresbury SuperSTEM. These show two separate nanopipes with nominal diameters (given by black arrows) of 4nm (Figures 4(a-c)) and 7nm (Figures 4(d-f). The results show HAADF and the corresponding bright field images. The atomic structure is resolved, although the image detail is less symmetrical than in Figure 3, probably owing to slight specimen misalignments from the exact [0001] orientation. Figure 4 also shows EELS line profiles taken along the horizontal lines indicated. The line profiles compare the Ga-$M_{2,3}$, N-K and O-K edge signals. In all cases, the background was removed by using a power law fit to the pre-edge curve, and the remaining counts integrated over an extended energy window extending at least 20eV from the onset of the edge. In order to compare the curves, the Ga and N signals have been scaled to be in the ratio 1:1 far from the nanopipes, and the O signal has then been scaled to the N signal by using the relative K-shell cross-sections [13]. The curves, therefore, show relative atomic ratios for Ga, N and O.

Deleted: 0

Deleted: similar

Deleted: , along with

Deleted: 1

3. Interpretation of results

The results in Figure 1 demonstrate that the structure of individual nanopipes can vary considerably. The interpretation of the results in Figures 3 and 4 is, therefore, complicated by the fact that we cannot assume the nanopipe surfaces are perfectly edge-on. This is in keeping with the observation that there are changes in contrast over a transition region up to 1-2nm across, where the structure appears unchanged from the bulk. This is seen most clearly in Figure 3, and implies the presence of facets which are inclined to the beam direction. There is also some evidence for additional disordered material in the centre of nanopipes. This is most clearly visible in the bright field images of Figure 4(c,f). We believe this is due to carbon-based contamination, which is consistent with the presence of a carbon K-edge observed in the EELS spectra. The amount of disordered material and the carbon K-signal increased with increasing irradiation time, as expected from contamination.

The images therefore imply that the appearance of oxygen in the EELS linescans in Figure 4 is not accompanied by a change in crystalline structure. The linescans in Figure 4 suggest that the nanopipe in Figure 4(a-c) is partially constricted, since the Ga and N profiles do not fall to zero in the nanopipe centre. In contrast, the Ga and N profiles for the nanopipe in Figure 4(d-f) fall close to zero, suggesting an open core in this case. This is consistent with the HAADF and bright field images taking into account the presence of contamination. The EELS profiles for both nanopipes suggest that oxygen is present close to the nanopipe surfaces. The depth to which oxygen penetrates is not clear, owing to the surface faceting. However, we can take the minimum width of the oxygen peak as an upper limit. The oxygen profile in figure 4(d) suggests this limit to be about 2nm. By integrating the area under the oxygen peaks, we can, however, estimate the total amount of oxygen. This gives 1.9 ± 0.4 monolayers in Figure 4(a) and 1.8 ± 0.7 monolayers in Figure 4(f).

The presence of oxygen on the nanopipe surfaces may, of course, indicate surface oxidation. However, GaN is fairly inert, and the thermal oxide thickness has been measured to be much less than 1 monolayer [14]. Oxygen could also be introduced by pipe diffusion from the sapphire substrate (Al_2O_3), or from the plasma cleaning gases (25% O_2). The former is unlikely, given that the results were independent of the GaN deposit thickness (up to 55μm). Samples examined in the STEM prior to plasma cleaning also showed a substantial oxygen peak, although contamination ruled out quantitative analysis in this case. Thus, the results imply that significant oxygen has been introduced during growth. This is consistent with secondary ion mass spectrometry (SIMS) data, which implies that HVPE films, from the same source as ours, typically contain an oxygen concentration of greater than $10^{17}cm^{-3}$ [15]. The source of this oxygen is believed to be the feed gases.

The driving force for oxygen segregation to nanopipes needs discussion. Firstly, total energy calculations imply that oxygen is more favourable on {10-10} surfaces than on the (0001) surface owing to the formation of O_N-V_{Ga} complexes [16]. This implies that nanopipes, once formed, should act as a sink for oxygen through surface diffusion. We believe volume diffusion is not an additional factor. In contrast to surface diffusion, volume diffusion would lead to preferential absorption of oxygen (an oversized atom [17]) at edge and mixed dislocations owing to the elastic interaction between the oxygen and the dilatational part of the strain field associated with the edge component of the Burgers vector. Such a process accounts for the segregation of Mg to edge and mixed dislocations in AlGaN films, leading to these

Deleted: since

Deleted: 2

Formatted: Subscript

Formatted: Subscript

Formatted: Subscript

Deleted: ,

Deleted: 3

Deleted: 4

Deleted: 5

dislocations becoming open core [4]. In our case, EELS studies showed no clear evidence for segregation of oxygen to edge and mixed dislocations, and moreover these dislocations were of closed core type.

It is conceivable that the presence of oxygen on the {10-10} surfaces of nanopipes lowers the surface energy sufficiently to allow open core dislocations to form by the Frank mechanism. This, however, appears unlikely to be critical factor, given the evidence that nanopipes can also form without dislocations (Figure 1(c)). Alternatively, we believe that nanopipes may grow from surface pits generated during film growth, as envisaged schematically in Figure 5. As confirmed by atomic force microscopy (AFM) studies, surface pits on freshly grown GaN surfaces are preferentially associated with threading dislocations. These are largest for screw or mixed dislocations but small pits (around 0.5nm) are also believed to be associated with dislocations of edge type [18]. We believe therefore that oxygen segregation may stabilise these pits, which subsequently develop into nanopipes. One possibility is that the complete substitution of the surface nitrogen by oxygen, which is consistent with our results, allows nanopipe growth by inhibiting growth of GaN on the sidewalls (Figure 5(right)). Given that oxygen is a trace impurity, it may be that there is insufficient oxygen to maintain sufficient flow to a growing nanopipe, such that the inclined surfaces of nanopipes become temporarily depleted of oxygen. Under such conditions the nanopipe may close up before the concentration of oxygen recovers to a sufficient level. This could result in periodic fluctuations in nanopipe diameter, as envisaged in Figure 5(left), c.f the nanopipe imaged in Figure 1(b). Alternatively such periodic structures may be due to a post-growth instability [19]. The fact that nanopipes are associated with screw but not with edge and mixed dislocations needs explaining, as the latter dislocations are also associated with pits during growth. It

Deleted: 3

Deleted: m

Deleted: , in particular those with screw character

Deleted: 6

Deleted: 7

appears plausible, as suggested by Cherns et al [2], that the presence of atomic steps, of height a, which must be present on {10-10} surfaces for edge and mixed dislocations (i.e. defined by the Burgers circuit), but not on the corresponding surfaces for screw dislocations or dislocation-free nanopipes, may act as nucleation sites for continued GaN growth. In this case, these nanopipes would have a mechanism to grow out.

Deleted: 1

The presence of oxygen at the cores of dislocations in GaN is very significant in understanding their electronic properties. If our segregation argument is correct, some oxygen should be present at all types of dislocation. This remains to be confirmed for edge and mixed dislocations (n.b. impurity segregation has been considered as a factor in the dissociation of mixed dislocations reported recently [1]). In the case of the open core screw dislocations, our results show no evidence that the structure of the GaN changes at the nanopipe surfaces. There is also no evidence, from our work or that of others, of structural changes at the cores of edge and mixed dislocations. Thus, if, as this implies, oxygen is present and substitutes nitrogen, charge neutrality requires the presence of Ga vacancies. The resulting O_N-V_{Ga} complexes have been identified as deep acceptors in GaN. These acceptors should become negatively charged in n-doped material where the Fermi level is near the conduction band edge. This is confirmed by electron holography observations which show that dislocations in n-GaN are highly negatively charged [20, 21].

Deleted: observation

Deleted: O

Deleted: 18

Deleted: 19

Conclusions

The EELS studies discussed here suggest that oxygen segregates to the cores of dislocations in GaN grown by HVPE. It has been argued that the presence of the oxygen provides a mechanism for the formation of hollow cores. The results therefore confirm growing evidence that the formation of hollow core dislocations in GaN is impurity related, rather than an equilibrium configuration driven by the Frank mechanism.

The results imply that the core structure of dislocations in GaN, and thereby their electronic properties, can be altered by controlling impurity levels, an area which merits further work.

Acknowledgements

We are grateful to D. Look of Semiconductor Research Centre, Wright State University and R. Molnar of Lincoln Laboratory, MIT, for providing the samples, and for the use of the SuperSTEM (Dr A Bleloch), and an FEI Titan 80-300 TEM (Dr B Freitag). We are also grateful to the US Office of Naval Research (Dr Colin Wood) for financial support under grant #N00014-03-1-0579

References

1. I. Arslan, A. Bleloch, E.A. Stach and N.D. Browning, Phys. Rev. Lett. **94**, 025504 (2005)
2. D. Cherns, W. T. Young, J. W. Steeds, F. A. Ponce and S. Nakamura, J. Cryst. Growth **178**, 201-206 (1997)
3. D. Cherns, Inst. Phys. Conf. Ser. No. **169**, 241-250 (2001)
4. D.Cherns, Y.Q. Wang, R. Liu and F.A. Ponce, Appl. Phys. Lett **81**, 4541-4543 (2002
5. M.Q. Baines, D. Cherns, J.W.P. Hsu and M.J. Manfra, MRS Proc. Vol **743** Paper L2.5 (2002)
6. F.C. Frank, Acta Cryst. **4**, 497 (1951)
7. W. Qian, M. Skowronski, K. Doverspike, L.B. Rowland and D.K. Gaskill, J. Cryst. Growth **151**, 396 (1995)
8. J. Heindl, W. Dorsch, H.P. Strunk, St. G. Müller, R. Eckstein, D. Hofmann and A. Winnacker, Physical Review Letters 80, 740 (1998)
9. J.E. Northrup, Appl. Phys. Lett. **78**, 2288 (2001)
10. I. Arslan and N.D. Browning, Phys. Rev. Lett. **91**, 165501 (2003)
11. M.E. Hawkridge and D. Cherns, Appl. Phys. Lett. 87, 221903 (2005)
12. D. Cherns and A. R. Preston, J. Electron Microscope Technique **13** , 111 (1989)
13. R.F. Egerton, "Electron Energy-Loss Spectroscopy In The Electron Microscope", Plenum Press, second edition 1996
14. N.J. Watkins, G.M. Wicks and Y. Gao, Appl. Phys. Lett. 75, 2602-2604 (1999)
15. X.L. Sun, S.H. Goss, L.J. Brillson, D.C. Look and R.J. Molnar, J. Appl. Phys. 91, 6729-6738 (2002)

Formatted: Font: Bold
Formatted: Bullets and Numbering
Formatted: English (U.K.)
Formatted: Font: Bold
Formatted: English (U.K.)

16. Elsner J, Jones R, Haugk M, Gutierrez R, Frauenheim T, Heggie MI, Oberg S, Briddon PR Appl. Phys. Lett. 73, 3530-3532 (1998)

17. T. Mattila and R. M. Nieminen, Phys. Rev. B 54, 16676–16682 (1996)

18. P. J. Hansen, Y. E. Strausser, A. N. Erickson, E. J. Tarsa, P. Kozodoy, E. G. Brazel, J. P. Ibbetson, U. Mishra, V. Narayanamurti, S. P. DenBaars, and J. S. Speck, Appl. Phys. Lett. 72, 2247 (1999)

19. F. Pailloux, J. Colin, J.F. Barbot and J. Grihle, Appl. Phys. Lett. 86, 131908 (2005)

20. D. Cherns and C.G. Jiao, Phys. Rev. Lett. 87 (20), 5504-5507 (2001)

21. D. Cherns, C.G. Jiao, H. Mokhtari, J. Cai and F.A. Ponce, Phys. Stat. Sol. B 234, 924-930 (2002)

Figure Captions

Figure 1: Bright field images of nanopipes in a 5µmGaN/sapphire cross-sectional sample, with the growth surface uppermost, (a) nanopipe with uniform cross-section; image taken under near two-beam conditions with g = 0006, (b) nanopipe consisting of pyramidal voids with apices pointing downwards in the [000-1] direction towards the substrate; imaging conditions as for (a), (c) an irregular nanopipe, *b*, associated with a dislocation leading to changes in diffraction contrast, and a nanopipe, *n*, which has no dislocation and shows no change in diffraction contrast; many beam imaging conditions.

Figure 2: Bright field image of a 5µmGaN/sapphire cross-sectional sample. Sample bending has produced a g = 0004 diffraction contour which splits on crossing a nanopipe indicating the presence of an associated dislocation. The splitting suggests that the dislocation has a Burgers vector with a c-component.

Figure 3: HAADF image of a nanopipe in a plan-view plasma-cleaned 5µmGaN/sapphire sample taken at 300kV in a FEI Titan 80-300 TEM. The microscope was configured without an aberration corrector on the probe forming lenses [Courtesy of Dr B. Freitag, FEI].

Figure 4: STEM studies of nanopipes in plan-view samples subjected to plasma cleaning: (a-c) and (d-f) show nanopipes in a 0.6µmGaN/sapphire sample and 5µmGaN/sapphire sample respectively, (a,d) EELS line profiles taken along the lines

indicated in the HAADF images (b,e) with black and white arrows indicating corresponding points, (c,f) show corresponding bright field images.

<u>Figure 5</u>: Schematic showing a proposed model for nanopipe growth. The right hand side shows growth on the assumption that there is sufficient oxygen to substitute and stabilise the vertical nanopipe surfaces, and the left hand side envisages a more limited supply of oxygen leading to closure of the nanopipe as the oxygen becomes temporarily depleted.

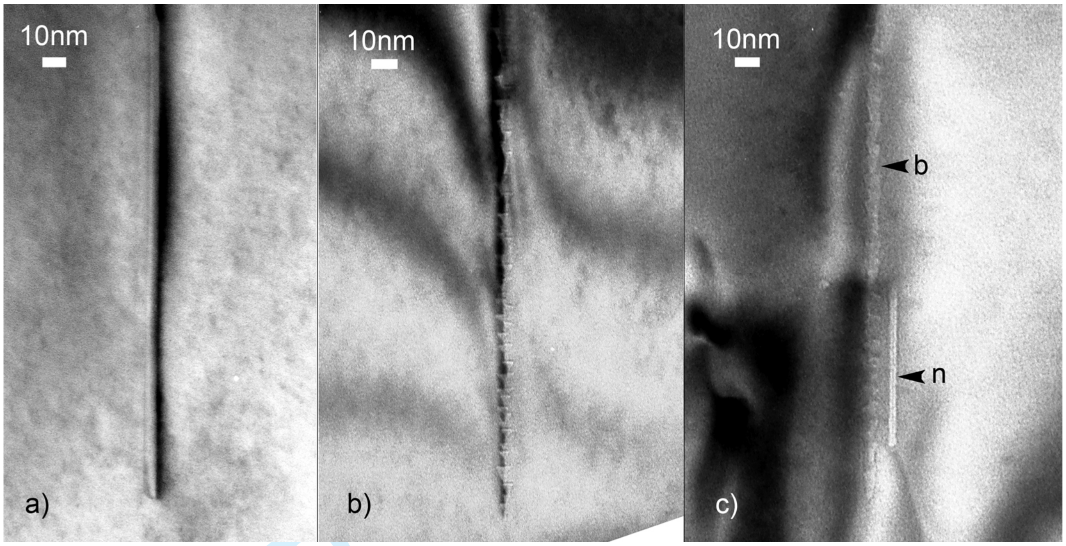

Figure 1

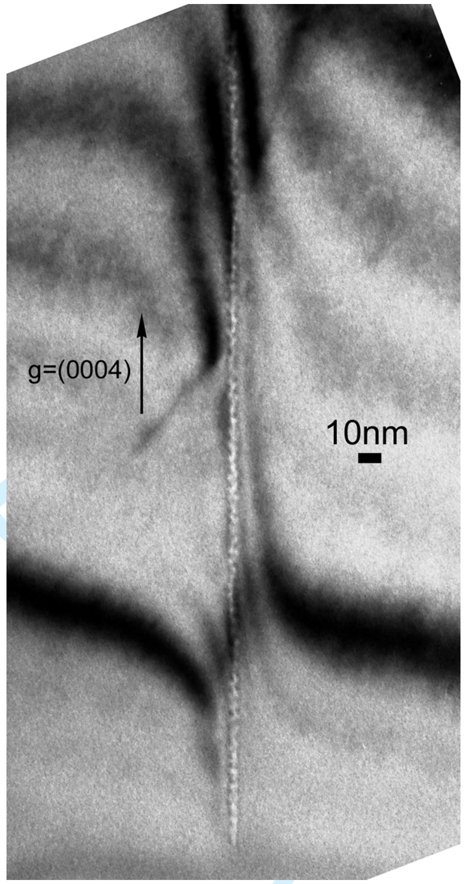

Figure 2

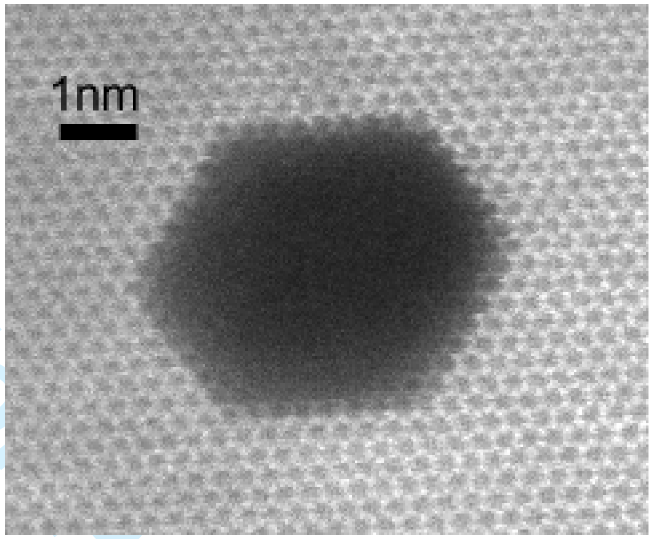

Figure 3

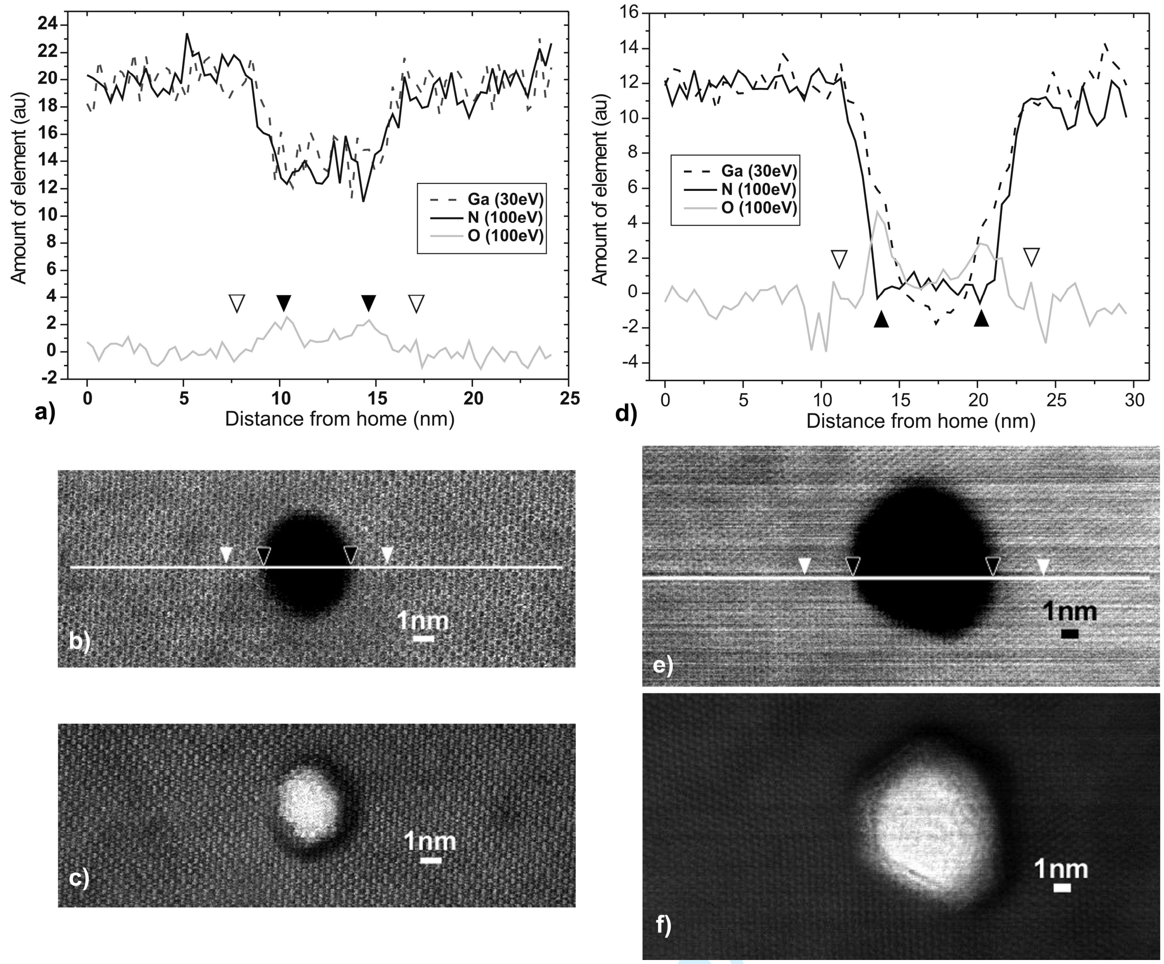

Amount of element (au)
Ga (30eV)
N (100eV)
O (100eV)
a)
Distance from home (nm)
d)
1nm
b)
c)
e)
f)

Figure 4

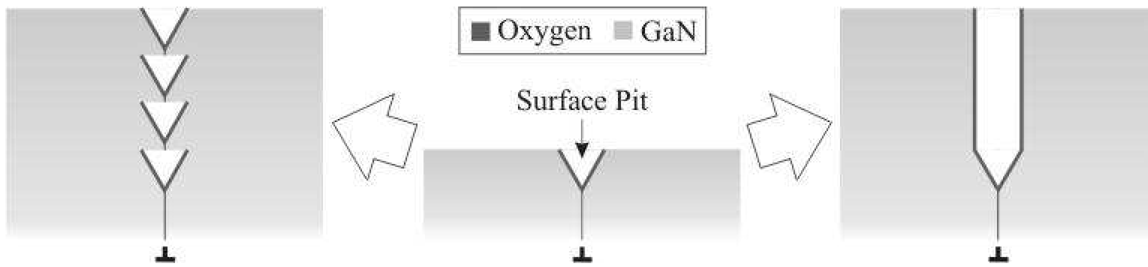

Figure 5